HHS Public Access

Author manuscript

Eur J Radiol. Author manuscript; available in PMC 2020 October 23.

Published in final edited form as:

Eur J Radiol. 2020 August ; 129: 109067. doi:10.1016/j.ejrad.2020.109067.

A review of optical breast imaging: Multi-modality systems for breast cancer diagnosis

Quing Zhu[a,b,*], **Steven Poplack**[b]

[a]Department of Biomedical Engineering, Washington University in St Louis, MO 63130, United States

[b]Department of Radiology, Washington University in St Louis, MO 63110, United States

Abstract

This review of optical breast imaging describes basic physical and system principles and summarizes technological evolution with a focus on multi-modality platforms and recent clinical trial results. Ultrasound-guided diffuse optical tomography and co-registered ultrasound and photoacoustic imaging systems are emphasized as models of state of the art optical technology that are most conducive to clinical translation.

Keywords

Ultrasound-guided diffuse optical tomography; Photoacoustic imaging; Co-registered digital breast tomosynthesis-diffused optical tomography; Co-registered MRI - diffused optical tomography; Breast cancer diagnosis

1. Introduction

Multiple imaging modalities are currently used for breast cancer screening and diagnosis. X-ray mammography is the predominant imaging modality for both screening and diagnostic imaging [1,2]. Screening mammography has been shown to reduce breast cancer mortality on the order of 15–45 % [3–6], but has diminished sensitivity in the setting of radiographically dense breast composition [7]. Breast US is widely used in diagnostic imaging and has been advocated for supplementary screening in average risk women with dense breasts, resulting in incremental cancer detection (ICDR) of 2–7 cancers per 1000 women screened [8–10]. Functional modalities including molecular breast imaging (MBI), contrast enhanced mammography (CEM), abbreviated MRI (ABMR) and traditional MRI have demonstrated even higher incremental cancer detection rates of 8–18 cancers per 1000 women, in supplementary screening of the dense breast [11–15]. Established breast imaging modalities are also disadvantaged by overdiagnosis, and low positive predictive values [16–18]. In the United States alone over 1 million biopsies are performed annually with a

*Corresponding author at: Department of Biomedical Engineering, Washington University in St Louis, MO 63130, United States. zhu.q@wustl.edu (Q. Zhu), poplack@wustl.edu (S. Poplack).

Declaration of Competing Interest

None.

positive predictive value of a biopsy recommendation estimated at 25 % and 30 % for screen detected and clinical breast abnormalities respectively [18].

Like MBI, CEM and MRI, optical imaging provides functional information about the vascular environment of a breast abnormality, and thereby has the potential to recognize biologically active disease, i.e. limit overdiagnosis, and improve diagnostic accuracy above that of anatomical imaging techniques like X-ray mammography or US. Furthermore, unlike established vascular based imaging techniques, it does not require intravenous injection, does not emit ionizing radiation, has very low medical risk, is intrinsically lower cost (than MBI or MRI) and is easily adaptable to the clinical imaging environment.

In the broadest sense optical breast imaging involves the transmission of light into the breast. Historically, diffuse optical imaging originated as breast trans-illumination, whereby a surface of the breast was subjected to a point source of broad spectrum “white” light and light transmitted through the breast was displayed. In 1929 Cutler reported the first clinical experience of trans-illumination of the breast in a series of 174 lesions and described characteristic findings in 8 different pathologic entities and clinical presentations [19]. A representative trans-illumination image of a solid tumor published in 1931 by Cutler is shown in Fig. 1 [20]. However, simple trans-illumination was limited by the ability of broad spectrum light to penetrate breast tissue, which was addressed by narrowing the wavelengths of transmitted light to the Red and Near Infrared (NIR) spectra [21,22]. Optical breast imaging evolved with further improvements in spectral narrowing by utilizing specified wavelengths of light that are selectively absorbed by different tissue components, and through light propagation modelling, i.e. improving the accuracy of mapping tissue components within the path of transmitted light by computer modeling and reconstruction of the absorption and scattering properties of the intervening tissue. In this way, four major tissue components can be quantified, including: water, fat, and oxygenated and deoxygenated hemoglobin [23,24]. In the case of Diffuse Optical Spectroscopy (DOS) and Diffuse Optical Tomography (DOT), NIR light at specified wavelengths is transmitted into the breast through optical ‘transmit’ fibers and the emitted light (both transmitted and scattered) is detected by a series of optical ‘receive’ fibers [25,26].

The photoacoustic effect - the conversion of light to sound - was first described by Bell in the late 1800’s [27]. In the last decade, with advances in lasers, ultrasound transducers, and tomographic reconstruction techniques, researchers have explored this principle for medical imaging purposes and the field has seen immense growth [28–33]. In contrast to diffuse optical imaging, Photoacoustic Imaging (PAI) transmitted NIR light is absorbed by tissue causing thermoelastic expansion and resulting in the emission of an acoustic pressure wave that is detected by an ultrasound transducer.

Both optical techniques provide useful clinical information by identifying breast abnormalities with increased total hemoglobin, which serves as a surrogate for increased and or altered vascularity. Due to wavelength specific absorption, DOS/DOT can quantify the total hemoglobin (THb), oxygenated hemoglobin and deoxygenated hemoglobin of tissue. Similarly, if two or more optical wavelengths are used, photoacoustic waves can be used to compute distributions of relative hemoglobin concentrations and blood oxygen saturation

(sO2). In general, breast cancer has higher THb than benign abnormalities or normal breast tissue [34,35], likely reflecting tumor angiogenesis. As tissues transform from hyperplasia to atypia to in situ carcinoma to invasive carcinoma, the increased metabolic needs create hypoxia and engender angiogenesis [36,37]. In support of this hypotheses, significant correlations between THb and markers of tumor angiogenesis have been demonstrated in patients with invasive breast carcinoma undergoing preoperative systemic therapy [38]. Greater metabolic need may also explain optical results of lower oxygen saturation, i.e. higher proportions of deoxygenated hemoglobin than oxygenated hemoglobin, in metabolically active conditions [35]. In the body of this review, we briefly discuss the physical principles of optical imaging and summarize the technical advancements of DOT and PAI including the combination of conventional imaging and optical imaging modalities. We present the most impactful clinical trial results for each multi-modality optical technology. Finally, we focus on US-guided DOT and co-registered US-PAI approaches as models of state of the art optical technology that are conducive to clinical translation.

1.1. Physical principles and imaging

Light photons interact with tissue through absorption and scattering (see Fig. 2). Ballistic, snake and diffusive photons refer to pathways of photon transmission through tissue. Ballistic photons travel along a straight-line pathway without being scattered, snake photons travel a quasi-straight path with only a few scattering events, and diffusive photons travel a random zig-zag path with many scattering events. Certain molecules like oxygenated and deoxygenated hemoglobin absorb light at specified wavelengths and are termed chromophores (see Fig. 2 insert). Most of the received light emanates from scattering. Accurate recovery of tissue optical properties requires mathematical modeling of light diffusion through tissue [25] and benefits from a-priori knowledge of tissue composition and lesion location provided by conventional imaging modalities.

1.2. DOS - DOT

DOS measures the reflected photons from the incident NIR light on the tissue surface and fits tissue optical absorption and scattering properties based on light diffusion models [23], while DOT measures transmitted or reflected photons and uses tomography reconstruction algorithms to image spatial absorption and/or scattering distributions [25,39,40]. Reconstruction algorithms are largely based on the light diffusion equation, which is an approximation of photon transport in biological tissue. The reconstruction process recovers lesion optical absorption and/or scattering properties from either transmission and/or reflection measurements made at the tissue surface. DOS systems typically consist of several pairs of sources and detectors and are used to estimate average optical properties of biological tissue. The systems are simple and low cost, however, imaging capability is limited [23]. While DOT systems have 3-D image capbility and is presented in greater detail.

Four types of the DOT imaging systems have been developed based on different light source and detection techniques: time-domain (TD), frequency domain (FD), continuous wave (CW), and mixed FD and CW systems. The TD diffuse optical technique used a picosecond laser pulse to illuminate the tissue and the temporal distribution of received photons known as the temporal point spread function (TPSF) is collected from multiple detectors [41–43].

The differences between TPSFs and an external reference derived from the source directly provide photon time of flight profiles. These time-resolved spatial measurements acquired from the detectors can reveal the spatial distribution of breast lesions using tomographic techniques discussed later. Over the past two decades, the techniques have been advanced to clinical studies [43]. However, the complexity and high cost of the system have hampered the spread of the TD systems [42].

The FD system directly modulates the amplitude of the light source at a high frequency (> 50 Mhz), and detectors measure the reduction in amplitude and phase shift of the transmitted signal [44,45]. FD systems typically employ one modulation frequency and many light sources consisting of multiple wavelengths and many detectors of broader spectral and frequency bandwidths. The detected signal at each detector for each wavelength is compared with an external reference derived from the source directly to provide amplitude and phase measurements. These spatially resolved measurements at each wavelength acquired from all detectors can reveal the spatial distribution of breast lesions using tomographic techniques discussed in the following section. The cost of FD systems is significantly less than TD systems. Thus, FD systems have been widely used by researchers as well as industry. The CW system emits NIR light at a constant intensity or with a low frequency modulation (a few kHz) to improve signal to noise. Detectors measure the reduction in amplitude of the transmitted signals [46]. CW systems with multi-wavelength laser diodes and dense source and detector arrays have been developed and used for clinical studies [47–49]. Frequency domain systems require fast response rate detectors, typically photomultipliers or silicon avalanche photo-detectors as well as high frequency detection circuits. However, CW systems only require slow response rate photo-detectors and low frequency circuits. Therefore, CW system cost and complex is far less than FD systems. As a result, more sources and detectors have used in the CW systems [49]. However quantitative optical reconstruction using amplitude only data from CW systems is limited and clinical application has largely been confined to tracking dynamic changes in breast abnormalities [47,48]. FD and CW systems have been combined to overcome the reconstruction limitation of the CW systems and cost and complexity of FD systems [50].

Imaging reconstruction of unknown tissue optical absorption and scattering X (see Eqn.1) is largely based on inverse optimization methods which iteratively search the absorption and scattering distributions of the tissue while minimize the error between the measurements from the tissue, Y, and computed forward measurements $f(X)$. The forward measurements are based on models computed from TD, or FD, or CW diffusion equations. λ is a regularization matrix to mitigate the non-uniqueness or stability of the solution X. A stopping criterion is typically implemented to stop the iteration and obtain estimated absorption and scattering distributions X of the tissue. The hemoglobin distributions (oxygenated-, deoxygenated-, and THb) are computed from absorption distributions at the selected wavelengths based on known extinction coefficients of the wavelengths used [25,51],

$$Obj(X) = \arg\min_{X} \|Y - f(X)\|^2 + \|\lambda X\|^2 \quad (1)$$

1.3. PAI

PAI is a hybrid imaging technology that uses nanosecond laser pulses in the NIR range to excite tissue (see Fig. 3), which then undergoes thermoelastic expansion and generates heat that is dispersed as acoustic (or photoacoustic) waves. The acoustic wave is received and quantified by the US transducer array as an optical absorption distribution, which in turn reveals optical contrast. Optical contrast is directly related to microvascular networks and the distributions of relative hemoglobin concentrations and sO2 can be mapped when two or more optical source wavelengths are used. Photoacoustic tomography systems used for breast imaging can be categoried into two major configurations depending on light illumination methods and photoacoustic detection methods: photoacoustic tomography CT - PACT and photoacoustic tomography -PAT. In PACT, nanosecond pulses illuminate a wide-field and 2D cross-section images can be reconstructed from projections, similar to x-ray CT, received from a ring transducer array or a linear or a curved linear array around the breast. 3D volumetric images can be obtained when the transducer is mechanically translated or arranged to acquire data spatially in 3D [30,52–56]. In PAT, nanosecond pulses illuminate a wide-field, commerical handheld transducers with a small field of view are used to acquire real-time 2-D images [35,57–61]. The penetration depth of PACT and PAT is tunable with ultrasound frequency. In the diagnostic ultrasound frequency range of 3–10 MHz, with a temporal resolution of 150–500 μm, the penetration depth of PAI in tissue can reach 3–4 cm or more in the near-infrared spectrum, depending on the laser power and the background tissue optical properties. However, because of the need of screening the entire breast in a PACT imaging set-up, the 3–4 cm penetration depth limits the PACT to closer to surface lesions. Currently, PACT requires laboratory prototypes of 2D array transducers. Related clinical studies are limited to pilot feasibility studies. However, PAT has advanced to a larger scale patient studies because it can readily use handheld US transducers and can be adopted to the breast imaging work flow. In this review, we will focus on PAT because it will have immediate impact on breast cancer diagnosis. We will use PAI to refer photoacoustic imaging in general, PACT to 3D volumetric imaging using 2D array transducers and PAT to 2D cross-section imaging using handheld transducers in the following manuscript.

There are advantages and disadvantages to each of the optical imaging technologies. The advantages of DOT are: 1) high sensitivity with no light to sound conversion loss; 2) the provision of quantitative optical properties for diagnosis; 3) no major safety considerations, i.e. DOT laser diodes have no vision risk unless viewed directly with naked eye; 4) capacity to image larger breast lesions; and 5) ready adaptation of US-guided DOT to existing clinical US systems. The advantages of PAT are: 1) high spatial resolution; 2) real-time qualitative image display, and 3) image presentation, i.e. lesion vasculature and sO2 can be superimposed on the gray scale US image to create a fusion image for interpretation, which is familiar and intuitive to radiologists.

Both technologies have limitations. The challenges for DOT include: 1) lower resolution due to intensive light scattering in tissue; 2) non-real time data processing and time-intensive tomographic image reconstruction; and 3) the need for a reference such as a calibration phantom or contralateral normal breast. The challenges for PAT are: 1) image features are qualitative and maybe subject to reader variability; 2) background tissue absorption may

produce confounding image artifacts; and 3) safety - PAI lasers require the operator and patient to wear protective eyewear; 4) clinical adaptability - currently PAT requires a separate US/PAT unit rather than adaptation of available clinical equipment.

1.4. Multimodality co-registered optical imaging

DOT and PAI systems utilize a similar variety of breast positioning and imaging array geometries for data acquisition and imaging formation. DOT was initially developed as a standalone technology and deployed in three different delivery systems. Standalone DOT systems either sandwiched the breast between two parallel plates, with sources and detectors deployed on opposite sides of the breast [45,62–65], used a cup-like geometry with the patient prone and the breast pendant in a fluid medium or in close contact with sources and detectors [48,66–68] or performed with a hand-held probe containing optical source and detectors, utilizing a reflection geometry [69–71]. However, it was widely appreciated in early 2000 that standalone DOT systems could not compete in terms of spatial resolution with x-ray, ultrasound and MRI but offer unique functional information critical for diagnosis of tissue malignancy.

PACT was also developed as a standalone system using similar breast positioning geometries: prone positioning with the pendant breast lightly compressed in a planar (mammography like) geometry, prone pendant breast lightly compressed within a hemi-cylindrical cup, prone non-compressed breast with a radial (spherical or hemispherical) acquisition [30,52–56]. In the prone position, the pendant breast is illuminated from the bottom while in the planar geometry, the breast is illuminated from either one side of the compressed breast or both sides of the breast. These standalone systems are capable of providing high-resolution 3D volumetric images, however, with slow data acquisition due to mechanical scan of the transducers. Further technology developments are needed to advance PACT systems for breast cancer screening. In the hand-held imaging geometry, the patient is in supine positioning with the breast illuminated from both sides of a one dimensional handheld linear US array [57–61]. The B-scan PAT images can be formed in real-time by using delay-and-sum or back-projection imaging algorithms. The B-scan PAT images can be superimposed on B-scan US images for co-registration. Due to the limited field of view of the transducer, the resolution of these PAT systems are limited to depth-dependent US resolution.

Reconstruction of DOT represents a typical ill-posed inverse problem of a large number of imaging voxels with unknown optical properties and a relative limited number of measurements. This necessitates the incorporation of *a priori* information of tissue composition and lesion location from other high resolution imaging modalities into the DOT inverse problem in order to obtain an accurate and viable solution [72–74]. Approaches include using anatomical information obtained from high resolution imaging modalities to 1) segment the imaging volume into a lesion region(s) and a background tissue region (s) to reduce the number of voxels with unknown optical properties X in the forward model $f(X)$ [72]; and 2) use directly segmented imaging volume or high resolution gray scale images to impose regularization $\boldsymbol{\lambda}$ in the reconstruction given in Eqn.1 [73,73,74]. Additionally, the multi-modality approach incorporates complementary anatomic (i.e. structural) information

from conventional imaging with physiologic (i.e. functional) information from optical imaging. Three conventional breast imaging modalities have been co-registered with DOT, including digital breast tom synthesis [75–77], US [34,78–83] and MRI [84–87] (see Table 1). Recent system advancements include an MRI-guided wideband (660–948 nm), hybrid FD and CW optical spectral tomography system [50], a tomosynthesis coupled NIR spectral tomography system for dual-modality breast imaging [88], a 3-D co-registered tomosynthesis and dynamic DOT system [89], and a compact co-registered US-guided DOT system [90]. The conventional high resolution imaging modality routinely used in clinics localizes a pre-defined imaging abnormality as the region of interest (ROI) in a co-registered imaging set-up. The reconstruction algorithm either segments the ROI from background or impose regularization in reconstruction, allowing for more accurate recovery of optical parameters within the abnormality and improving breast lesion diagnostic accuracy.

Unlike DOT, PAI intrinsically involves two modalities: NIR light transmission and absorption to create photoacoustic waves and US to receive the emitted photoacoustic waves. Image contrast relates to tissue optical properties while image resolution depends on US. Despite the intrinsic utilization of US, the early PACT systems were essentially standalone devices and did not utilize clinical imaging modalities to localize or define an anatomic region of interest [33]. The subsequent addition of a localizing modality, i.e. gray scale US [35,61], allows for anatomic-optical image fusion for interpretation.

2. Clinical results

2.1. Co-registered digital breast tomosynthesis (DBT) -DOT

Shortly after the development of DBT prototypes in the late 1990’s, co-registered DBT DOT systems were created with 2 goals in mind, (1) improving DOT reconstruction algorithms by providing a priori structural information from DBT, and (2) enhancing diagnostic accuracy of DBT by adding functional information gleaned from DOT. Early co-registered DOT-DBT system trials were designed to establish system feasibility and to benchmark optical parameters in the setting of X-ray mammography compression [91,92]. Two groups of investigators, i.e. from Massachusetts General Hospital (MGH) and from Thayer School of Engineering at Dartmouth College independently developed systems using General Electric and Hologic DBT systems respectively. Fang and colleagues from MGH reported that an average THb and sO2 of 16.2 μM and 71 %, respectively in 68 “healthy” breasts, where the THb showed a linear trend with breast density. The authors concluded that the low THb value compared to the existing optical literature was likely due to mammographic compression. Michaelson and colleagues from Dartmouth studied 27 women with normal mammography and varied breast composition demonstrating correlations between breast composition (i.e. radiographic breast density) with THb ($r = 0.64$, $p = 0.001$), water ($r = 0.62$, $p = 0.003$), and lipid concentrations ($r = -0.74$, $p < 0.001$), but not with sO2 [75]. Comparison of compressed and minimally compressed acquisitions showed a significant decrease in sO2 due to compression (58 % versus 50 %, $p = 0.04$).

In 2011, Fang and colleagues demonstrated significant differences in optical properties between malignant and benign - normal women. In a study of 189 breasts in 125 patients, including 138 normal breasts and 51 breasts with imaging abnormalities [76], bulk THb

correlated with fibroglandular tissue fraction (Fg), R = 0.57, p < .0001 and the THb of 26 malignant tumors ranging from 0.6 to 2.5 cm was significantly greater than 17 solid benign lesions (p = .025), 8 cysts (p = .0033), and fibro-glandular tissue of the same breast (p = .0062). This group has since expanded the system to a dynamic DOT apparatus designed for tight integration with commercial DBT scanners and providing a fast (up to 1 Hz) image acquisition rate to enable tracking hemodynamic changes induced by the mammographic breast compression [89].

Based on these studies, it is now accepted that THb is lower in the compressed state, correlates with breast density and has the capacity to differentiate malignancy.

2.2. Co-registered MRI - DOT

The first clinical study of MRI-guided DOS was reported by Ntziachristos and colleagues [84]. The breast was compressed softly between two plates, which contained both optical fibers and radio-frequency coils for co-registration. A TD system was used to deliver two to three NIR wavelengths to 24 optical fibers with 8 optical detectors within a detection plate. Both source and detector optical fibers were 10 m long so that the DOT system could avoid interference with the MR scanner. The hybrid system utilized MR structural images as a priori information and quantified the hemoglobin of five malignant and nine benign breast lesions in vivo. In general, malignant abnormalities had lower sO2 and higher hemoglobin concentration than benign lesions. The average THb concentration and sO2 of the malignant lesions was 130 ± 100 μM, and 60 ± 9 % respectively. Fibroadenomas exhibited lower THb of 60 ± 10 μM and a mild level of higher sO2 of 67 ± 2 %, and normal fibroglandular tissue had low THb of 18 ± 5 μM and higher sO2 of 69 ± 6 %.

Brooksby and colleagues from Dartmouth in 2006 developed a broadband MRI guided DOT system with 6 laser diode source fibers and 15 detector fibers distributed in a ring structure and reported results on 11 normal subjects [85]. The ring system was located inside the open breast MRI coil to allow positioning along the length of the pendant breast. The entire data acquisition occurred in less than 10 min. Subsequently this group studied a larger cohort of 44 patients with breast abnormalities using a system with three additional CW optical wavelengths and photodiode detectors [93]. In a subset of 30 exams that met optical data sensitivity criterion, the MR-guided DOT separated malignant from benign lesions using THb ($p < 0.01$) and tissue optical index (TOI) defined as THb × water/Lipid (TOI, $p < 0.001$). Combined MRI plus TOI data produced the best diagnostic performance.

In a recent study reported by the same group in 2017 [94], twenty-four subjects with 16 malignant and 8 benign abnormalities were simultaneously imaged with MRI including T2 weighted, diffusion weighted (DWI) and dynamic contrast enhanced sequences (CEMRI) and DOT prior to biopsy. DOT was guided by both CEMRI and non-contrast MRI using the T2 weighted sequence for guidance. MRIs were evaluated independently by three breast radiologists blinded to the subsequent pathology results. Optical image reconstructions were constrained by grayscale values in the T2-MRI. MRI and optical images were used, alone and in combination, to estimate the diagnostic performance of the data. Operating characteristics were described for CEMRI alone, non-contrast MRI -guided DOT, and CEMRI-guided DOT. The authors found that the most accurate results occurred when

combining non-contrast (T2-DWI) MRI with T2-guided optical imaging (Table 1), suggesting that similar or better diagnostic accuracy can be achieved without requiring a contrast agent. Table 1 summaries the outcome measures and key results of DBT and MRI guided DOT for clinical trials with more than 20 patients.

Co-registered MRI - DOT, especially with the innovation of T2 weighted MRI guided DOT, shows promise in distinguishing breast cancer, but has only been evaluated in a few small pilot studies. It has the potential to address the specificity limitations of breast MRI. However, it brings the additional challenges of incorporating optical fibers into the MRI gantry and either creating MRI compatible equipment or extending optical fiber length to allow the optical console to be located outside of the high magnetic field. Coupled with the MRI disadvantages of limited access and high expense make co-registered MRI-DOT less likely for near term clinical implementation.

2.3. US-guided DOT

The first US-guided DOT patient study was reported by Zhu et al. in 2003 [78]. A 1st generation US-guided frequency-domain DOT prototype system fit a commercial US transducer within a clamshell like optical probe consisting of 12 dual-wavelength (780 nm and 830 nm) optical couplers and 8 detection fibers. US identified the imaging abnormality and DOT simultaneously mapped hemoglobin content. Each co-registered data set was acquired in approximately 2–3 seconds. Initial findings of two studies using this system involved 100 imaging abnormalities in 84 patients, including ten early stage invasive carcinomas and 90 benign lesions [78,79]. The malignant abnormalities had about two-fold greater total hemoglobin concentration than benign abnormalities ($p < .001$) and had a localized THb distribution as compared to a more diffuse distribution on THb distribution maps. US-DOT substantially outperformed color Doppler US [79].

Subsequently, two larger-scale trials were conducted in 466 women undergoing image guided needle biopsy and utilizing 2nd and 3rd generation US-guided frequency-domain DOT prototype systems and results were reported in 2010 and 2016 publications [34,80]. The 2nd generation prototype had two laser diodes (optical wavelengths of 780 nm and 830 nm), while the 3rd generation prototype had 4 laser diodes (wavelengths of 740 nm, 785 nm, 808 nm and 830 nm). In both systems, light was delivered to 9 source locations on the probe and was received by 10 photomultiplier detectors with parallel electronic channels. Optical absorption distributions at each wavelength were reconstructed, and THb was computed from the absorption maps. Both studies again demonstrated significantly higher THb in malignant (than benign) abnormalities and showed differences between lower stage (Tis-T1) vs. higher stage (T2–4) malignancies, Figs. 4 and 5 show typical examples of malignant and benign subjects. A characteristically malignant heterogeneous peripheral THb distribution pattern was identified in 38 % of T2–4 malignant lesions. The third generation system demonstrated moderate correlation between THb and both histological grade ($r = 0.283$, $p = 0.034$) and nuclear grade ($r = 0.315$, $p = 0.015$) (44). Similarly, maximum oxygenated hemoglobin correlated moderately with nuclear grade ($r = 0.267$, $p = 0.042$). Both studies also demonstrated different nm, 785 nm, 808 nm and 830 nm). In both disease categories and identified groups of benign pathology such as fibroadenomas, fat necrosis and

inflammatory conditions and proliferative diseases with and without atypia as a source of false positives.

In the final study, two radiologists retrospectively reviewed the US findings and reassessed each abnormality with a final BIRADS assessment. When a positive result was defined as THb > 80 μM or a BIRADS 4C or 5 assessment the sensitivity and NPV improved substantially with only a mild decrease in specificity and PPV. When a THb lower threshold (THb < 50 μM) was employed, biopsy recommendations for 4A and 4B lesions decreased by 50 % and 39 % respectively (an average of 45 %), while only a single malignant abnormality (i.e. 1 cm low grade invasive carcinoma) was misclassified by one reader.

Contemporaneously, several international investigator groups conducted clinical studies using a single integrated commercial system, OPTIMUS II™ (XinaoMDT Technology Co., Ltd., Langfan, China). The system incorporated a frequency domain DOT system consisting of two laser diodes (785 nm and 830 nm), 9 source locations and 10 avalanche photodiode detectors along with a commercial US system (Terason t3000 Ultrasound; Teratech Burlinton, MA USA). Related clinical studies involved approximately 1000 patients (Table 2).

The first study utilizing OPTIMUS II™ was performed on 198 women with 214 lesions [81]. The average THb was approximately twice as high and significantly greater in malignant than benign abnormalities (Table 2). Similar to prior reports [34,80], the authors described false positive results in fibroadenomas, papilloma, adenosis, benign phyllodes tumors and inflammatory conditions. In addition, each lesion was systematically classified as vascular or non-vascular by color Doppler US and malignant or benign by US-guided DOT based on THb. Thirteen of 118 (11 %) cancers were non-vascular but had elevated THb, while 25 of 96 (26 %) of benign lesions were vascular by color Doppler evaluation but had low THb. The investigators concluded that the addition of THb could be helpful for identifying suspicious nonvascular lesions and characterizing probably benign vascular lesions [95].

A second group of investigators evaluated the level of inter-observer agreement of conventional US combined with US-guided DOT (OPTIMUS II™) for differentiation of malignant and benign lesions in 121 patients [82]. In the final data analysis of 122 lesions interpreted by two radiologists there was almost perfect inter observer agreement in BIRADS final assessment with the combination of US and US-guided DOT (k = 0.8619) as compared with that of US only (k = 0.6574). However, the overall accuracy as noted by areas under the ROC curve did not show a significant difference between US and combined US and US-guided DOT.

The same group evaluated data derived from the OptimusII™ trial. In 207 consecutive women that underwent US-DOT, correlation between clinic-pathologic variables and THb was performed in a subset of 53 women with 65 invasive ductal carcinomas [96]. In univariate analysis HER2 positivity, tumor size, and Ki-67 positivity were significantly correlated with maximum THb ($p < 0.05$). In multivariate analysis including tumor size, and ER, PR, HER2, and Ki-67 status, HER2 positivity correlated with maximum THb (p =

0.007). Recently, the same group also evaluated correlation of THb with pharmacokinetic features of Dynamic contrast-enhanced CE-MRI and pathologic markers of breast cancer in 37 patients with contemporaneous CE-MRI and US-DOT [97]. The parameters THb and MRI signal enhancement ratio showed marginal positive correlation ($r = 0.303$, $p = 0.058$).

A third group, reported their clinical experience with OPTIMUS in 136 lesions that underwent biopsy in 102 women, including 54 cancers and 82 benign abnormalities [83]. The operating characteristics of the combination of US and US-DOT was substantially improved from either technique alone. Recently, the same group evaluated associations of THb and clinicopathological parameters in 455 breast cancers in 447 patients using OPTIMUS-01HWS [98]. The authors found that the average THb was significantly greater in ER negative, PR negative than in ER positive, PR positive cancers ($p = .005$ and $p = .01$, respectively) and that cancers with axillary lymph node metastases or lymphovascular invasion also had higher average THb ($p = .042$ and $p = .043$, respectively). No significant differences in THb were found in groups of infiltrating vs. non-infiltrating, HER2+ vs. HER2−, Ki67 high vs. Ki67 low, and during different menstrual phases ($p = .457$, $p = .917$, $p = .417$, $p = .213$, respectively).

Based on these studies from multiple investigators with data obtained from different DOT systems, it is accepted that US-guided DOT demonstrates 1) statistically significant higher tumor vascular contrast in malignant breast lesions than that in benign lesions; 2) the vascular contrast is correlated with the tumor aggressiveness; and 3) the vascular contrast in certain benign lesions is much lower than others and can be used safely to reduce benign biopsies. However, in order to integrate US-guided DOT into the clinical breast study flow, the DOT system needs to be miniaturized and its data processing and image reconstruction speed need to be improved to near real-time operation.

2.4. Co-registered US and PAT

Early pilot clinical results of co-registered US-PAI included both mammography like and handheld geometries. In 2016 Asao et al. reported phantom results and showed feasibility in a single patient with invasive ductal carcinoma using a prone US-PACT system with the pendant breast compressed between parallel plates [99]. An US transducer scanned the breast horizontally translating vertically in 10 mm increments following each sweep. An example from this system is given in Fig. 6. Two small trials of co-registered US-PAT hand-held prototype devices reported in 2017 and 2018 demonstrated similar results [58,60]. Becker et al. imaged 6 healthy volunteers, 5 women with invasive carcinoma and 2 women with DCIS and demonstrated differences in hemoglobin and sO2 between invasive carcinoma and normal controls only [60]. Using a similar device Diot et al. showed increased tumor blood volume over background in ten patients with invasive carcinoma [58]. Dean-Ben et al. demonstrated that young healthy volunteers with fibroglandular-dominated dense breasts revealed the feasibility of rendering three-dimensional images representing vascular anatomy and functional blood oxygenation parameters at video rate [59].

Two larger scale industry sponsored prospective multicenter clinical trials of a commercial handheld PAT system (Imagio™ Seno Medical Instruments) were also published in 2017 and 2018 [35,100–102]. The co-registered device contains a clinical quality grayscale US

unit combined with an optoacoustic imaging component. One study was conducted from 2015 to 2016 in five centers in the Netherlands. The study was restricted to low to moderate suspicion masses (BIRADS 4A and 4B) and utilized all available imaging information [101]. The other trial was performed in 16 sites in the US from 2012 to 2015, included probably benign (BIRADS 3) masses with adequate follow-up and suspicious masses (BIRADS 4A, 4B, 4C and 5) with biopsy results, and assessments were based solely on imaging (gray scale and optoacoustic) from the investigational device [35]. The first 100 subjects from this trial seen at seven sites were used as a training set and subsequently reported results separately [100].

In the European multi-center trial, the authors assessed the ability of co-registered US-PAT to correctly downgrade benign masses assessed as low or moderate suspicion (BIRADS 4A or 4B) on the basis of conventional SOC ultrasound. Of 209 patients with 215 BIRADS 4A or 4B breast masses, co-registered US-PAT correctly downgraded 47.9 % of benign masses classified as low suspicion 4A and 11.1 % of masses classified as moderate suspicion 4B. Three of 67 (4.5 %) malignant masses were incorrectly downgraded, including two of seven low suspicion (BIRADS 4A) and one of 60 moderate suspicion masses (BIRADS 4B).

The goal of the larger US trial was to compare the diagnostic accuracy of co-registered PAT information with grayscale US alone in differentiating benign and malignant sonographically visible masses [35]. The Imagio™ system contains an ‘internal’ gray scale US transducer that meets state of the art clinical specifications and can be operated in gray scale only or duplex PAT/US modes. In the PAT/US mode, a two-laser system (1064 nm and 755 nm) and a hand-held US array (128 elements, 5 MHz) is used to create color coded hemoglobin maps fused with gray scale US images. The final reader study population included 1757 masses in 1690 subjects. Seven study readers blinded to conventional imaging and clinical data first evaluated US images from the ‘internal’ gray scale mode and then PAT/US images. In addition to BIRADS assessment and probability of malignancy, readers scored PAT data based on a set of five PAT imaging features: vessel score (internal vascularity and deoxygenation), blush score (volume averaging of unresolved vessels), hemoglobin score (internal hemoglobin signals), boundary zone score (external boundary vascularity and deoxygenation) and peripheral zone score (external peripheral radiating vessels) (Fig. 7). The specificity of PAT/US was 43.0 % versus 28.1 % for ‘internal’ gray scale US, yielding a statistically significant 14.9 % increase in specificity. There was a significant 2.6 % decrease in sensitivity: PAT/US = 96 % vs. internal US = 98.6 %. For benign masses read as BIRADS 3 by internal US, PAT/US resulted in appropriately downgrading 48.6 % (1023/2107) and inappropriately upgrading 21.3 % (48/2107). In the subset of BIRADS 3 with malignancy, PAT/US led to upgrading 47.0 % (31/66), while downgrading 27.3 % (18/66). The adjunctive use of PAT/US in the malignant population with ≥ BIRADS 4A gray scale US assessment resulted in upgrading 35.6 % (1415/3976) of malignant mass reads to a higher BIRADS category, while downgrading 3.9 % (157/3976) to a BIRADS 2 or 3. Correct upgrades were significantly higher than incorrect downgrades. Based on the five PAT/US imaging features, the related imaging scores were significantly lower in benign pathology than malignant pathology. In addition, the probability of malignancy increased with increasing feature score. Boundary and peripheral (rather than internal) scores were most highly correlated with malignancy.

Two subsequent studies derived from the initial 100 ‘training’ cases of the US multicenter Seno Medical trial were published in 2018 and also showed promising results [100]. In one trial sensitivity of PAT/US was unchanged from sensitivity of internal US (97.1 % vs. 97.1 %) while specificity with PAT/US improved to 44.3 % (vs. 36.4 % - gray scale US). In the other study PAT/US feature analysis again demonstrated higher scores for malignancy with external features more predictive than internal features.

Of note, readers in the three US multicenter clinical trials [35,100] were blinded to clinical information, such as clinical or mammographic findings, which likely negatively impacted accuracy. One might expect the additional clinical information to improve sensitivity and decrease specificity of the adjunctive PAT technology.

In addition to its demonstrated clinical impact on benign biopsy reduction, co-registered US - PAT has other desirable clinical features. As noted above, it has already been commercialized (Imagio™, Seno Medical Instruments) and thereby available for clinical implementation. The combined system conveniently allows for conventional US and PAT to be performed during the same exam. Furthermore, the optical parameters can be superimposed upon traditional US images to provide a fused image map (Fig. 5), providing a familiar image format for the interpreting radiologist. However, Imagio™ is an integrated US/PAT unit with special US transducer and hardware rather than an adaptation of available clinical breast US units. There is a huge challenge to replace commercial breast US systems with Imagio™and future clinical trials are needed to justify the added benefit.

3. Discussion

Conventional breast imaging with mammography and ultrasound has several important limitations, which create a niche for adjunctive imaging technologies like diffuse optical tomography and photoacoustic imaging. Optical imaging provides functional information on tumor related vascularity and generally demonstrates elevated THb and decreased sO2 in malignant masses. The combination of conventional imaging and optical imaging improves the optical imaging data and has the capacity for image co-registration.

All of the co-registered conventional - optical systems have advantages and disadvantages. Co-registered Digital Breast Tomosynthesis (DBT) -DOT can differentiate malignancy from benign abnormalities in designated regions of interest but has untapped potential as an adjunctive screening tool because the entire breast is included and screening with DBT is well established. However, more research is needed to confirm diagnostic accuracy in in the compressed state and novel designs and associated research is needed to assess a potential role in improving the accuracy of screening with DBT. Co-registered MRI - DOT has been shown to improve the diagnostic accuracy of breast MRI and has potential to improve the specificity of MRI, especially with the t2 weighted MRI guided DOT technique. However, due to its limited access and high cost, MRI is not used as a primary screening or diagnostic modality in breast imaging and more clinical studies are required to validate the potential benefit of co-registered DOT - MRI to justify the need. Furthermore there are logistical hurdles to create MRI compatible optical equipment.

Preliminary trials from both US-guided DOT and co-registered US-PAT demonstrate the ability to substantially (on the order of 45 %) reduce unnecessary biopsy of benign sonographically visible masses and thereby greatly improve the positive predictive value of a biopsy recommendation. If either or both technologies can be validated in phase 3 trials this could lead to significant reductions in the anxiety and minor morbidity related to a false positive biopsy recommendation and translate to substantial cost savings for patients, health care insurers and society at large. Furthermore encouraging data correlating optical parameters with markers of tumor biology are emerging.

The clinical adaptation of multi-modality optical breast imaging will depend on many factors, including the ability to maintain high sensitivity while reducing false positives, cost savings vs. additional system and exam costs, as well as acceptance by the breast imaging community. The technology for US-guided DOT and co-registered US-PAT techniques is maturing fast and clinical adoption of either one or both of the technologies may well come in the near future. Co-registered DBT-DOT will need further clinical studies to validate if optical contrast between malignant and benign breast abnormalities can be preserved under compression and therefore can be used synergistically with DBT to improve breast cancer diagnosis. Co-registered MRI - DOT will also need further clinical studies to validate the benefit of integrating an additional DOT system into the MRI for improving breast cancer diagnosis. PACT has a promise to be used as a standalone screening modality and further development is warranted to improve the data acquisition speed and also depth of penetration for breast cancer screening. The development of optical contrast agents is an active research area and has a great potential to improve cancer detection with a greater penetration depth for both DOT and PAI [103,104].

Lastly, same as the initial developments of x-ray, US, MRI and PET, optical imaging systems constructed by different research laboratories or companies have implemented different hardware, data processing, and imaging reconstruction software. As a result, it is difficult to perform cross-comparison of patient studies obtained from different systems. Currently, FDA is leading a significant effort to standardize optical imaging phantoms so different systems can acquire images of the same targets to perform cross-comparison [106]. With the further development of promising optical imaging technologies, the standardization of imaging systems should be followed for commercialization.

Acknowledgements

The authors gratefully acknowledge the funding support for the ultrasound-guided diffuse optical tomography project from the National Institutes of Health (R01EB002136, R01 CA228047). SPP acknowledges funding support from the Foundation for Barnes Jewish Hospital Ronald and Hanna Evens Endowed Chair in Women’s Health.

References

[1]. Sprague BL, Arao RF, Miglioretti DL, et al. National performance benchmarks for modern diagnostic digital mammography: update from the breast cancer surveillance consortium, Radiol 283 (2017) 59–69.

[2]. Schunneman HJ, Lerda D, Quinn C, et al. Breast Cancer screening and diagnosis: a synopsis of the European breast guidelines, AnnInternMed 172 (2020) 46–56.

[3]. Chen TH-H, Yen AM-F, Fann JC-Y, et al. Clarifying the debate on population-based screening for breast cancer with mammography A systematic review of randomized controlled trials on mammography with Bayesian meta-analysis and causal model, Medicine 96 (3) (2017) e5684. [PubMed: 28099330]

[4]. Moss SM, Nystrom L, Jonsson H, et al. The impact of mammographic screening on breast cancer mortality in Europe: a review of trend studies, J. Med. Scr 19 (Suppl. 1) (2012) 26–32.

[5]. Gabe R, Duffy SW, Evaluation of service screening mammography in practice: the impact on breast cancer mortality, Ann. Oncol 16 (Supplement 2) (2005) ii153–ii162. [PubMed: 15958448]

[6]. Coldman A, Phillips N, Wilson C, et al. Pan-canadian study of mammography screening and mortality from breast cancer, J. Natl. Cancer Inst 106 (11) (2014) dju261, 10.1093/jnci/dju261. [PubMed: 25274578]

[7]. Carney PA, Miglioretti DL, Yankaskas BC, et al. Individual and combined effects of age, breast density, and hormone replacement therapy use on the accuracy of screening mammography, Ann. Intern. Med 138 (2003) 168–175. [PubMed: 12558355]

[8]. Berg WA, Blume JD, Cormack JB, et al. Combined screening with ultrasound and mammography vs mammography alone in women at elevated risk of breast cancer, JAMA 299 (18) (2008) 2151–2163. [PubMed: 18477782]

[9]. Brem RF, Tabar L, Duffy SW, et al. Assessing improvement in detection of breast cancer with three-dimensional automated breast US in women with dense breast tissue: the somoinsight study, Radiol 274 (2015) 663–673.

[10]. Tagliafico AS, Airaldi S, Bignotti B, et al. Adjunct screening with tomosynthesis or ultrasound in women with mammography-negative dense breasts: interim report of a prospective comparative, Trial. J. Clin. Oncol 34 (2016) 1882–1888. [PubMed: 26962097]

[11]. Shermis RB, Wilson KD, Doyle MT, et al. Supplemental breast cancer screening with molecular breast imaging for women with dense breast tissue, AJR 207 (2016) 450–457. [PubMed: 27186635]

[12]. Sung JS, Lebron L, Keating D, et al. Performance of dual-energy contrast-enhanced digital mammography for screening women at increased risk of breast cancer, Radiology 293 (2019) 81–88. [PubMed: 31453765]

[13]. Bakker MF, de Lange SV, Pijnappel RM, et al. Supplemental MRI screening for women with extremely dense breast tissue, N. Engl. J. Med 381 (22) (2020) 2091–2102.

[14]. Kuhl CK, Schrading S, Stobel K, Abbreviated breast magnetic resonance imaging (MRI): first postcontrast subtracted images and maximum-intensity projection—a novel approach to breast cancer screening with MRI, J. Clin. Oncol 32 (2020) 2304–2310.

[15]. Comstock CE, Gatsonis C, Newstead GM, et al. Comparison of abbreviated breast MRI vs digital breast tomosynthesis for breast Cancer detection among women with dense breasts undergoing screening, JAMA 323 (8) (2020) 746–756. [PubMed: 32096852]

[16]. Puliti D, Duffy SW, Miccinesi G, et al. Overdiagnosis in mammographic screening for breast cancer in Europe: a literature review, J. Med. Screen 19 (Suppl. 1) (2012) 42–56.

[17]. Hubbard RA, Kerlikowske K, Flowers CI, et al. Cumulative probability of false-positive recall or biopsy recommendation after 10 years of screening mammography, Ann. Intern. Med 155 (8) (2011) 481–492. [PubMed: 22007042]

[18]. Lehman CD, Arao RF, Sprague BL, et al. National performance benchmarks for modern screening digital mammography: update from the breast cancer surveillance consortium, Radiol 283 (2017) 49–58.

[19]. Cutler M, Transillumination as an aid in the diagnosis of breast lesions, Surg. Gynecol. Obstet 48 (1929) 721–729.

[20]. Cutler M, Transillumination of the breast, Ann. Surg 93 (1) (1931) 223–234. [PubMed: 17866468]

[21]. Carlsen E, Diagn. Imaging 4 (28–34) (1982) 5.

[22]. Bartrum RJ, Crow HC, Am. J. Roentgenol 142 (1984) 409–414. [PubMed: 6607619]

[23]. Cerussi AE, Berger AJ, Bevilacqua F, Shah N, Jakubowski D, Butler J, Holcombe RF, Tromberg B, Sources of absorption and scattering contrast for near-infrared optical mammography, Acad. Radiol 8 (2001) 211–218. [PubMed: 11249084]

[24]. Tromberg BJ, Pogue BW, Paulsen KD, Yodh AG, Boas DA, Cerussi AE, Assessing the future of diffuse optical imaging technologies for breast cancer management, Med. Phys 35 (Junuary (6)) (2008) 2443–2451. [PubMed: 18649477]

[25]. Arridge SR, Methods in diffuse optical imaging, Philos. Trans. A Math. Phys. Eng. Sci 369 (November (1955)) (2011) 4558–4576, 10.1098/rsta.2011.0311 Review.

[26]. Fishkin JB, Gratton E, Propagation of photon-density waves in strongly scattering media containing an absorbing semi-infinite plane bounded by a straight edge, JOSA A 10 (1) (2020) 127–140.

[27]. Bell AG, On the production and reproduction of sound by light, Am. J. Sci s3–20 (118) (1880) 305–324.

[28]. Wang LV, Hu S, Photoacoustic tomography: *in vivo* imaging from organelles to organs, Science 335 (6075) (2012) 1458–1462. [PubMed: 22442475]

[29]. Oraevsky AA, Karabutov AA, Optoacoustic tomography, in: Vo-Dinh T (Ed.), Biomedical Photonics Handbook, CRC, Boca Raton, Fla, 2003.

[30]. Kruger RA, Kuzmiak CM, Lam RB, Reinecke DR, Del Rio SP, Steed D, Dedicated 3D photoacoustic breast imaging, Med. Phys 40 (11) (2013) 113301. [PubMed: 24320471]

[31]. Attia ABE, Balasundaram G, Moothanchery M, Dinish US, Bi R, Ntziachristos V, Olivo M, A review of clinical photoacoustic imaging: current and future trends, Photoacoustics. 16 (November 7) (2019) 100144, 10.1016/j.pacs.2019.100144 eCollection 2019 Dec. [PubMed: 31871888]

[32]. Steinberg I, Huland DM, Vermesh O, Frostig HE, Tummers WS, Gambhir SS, Photoacoustic clinical imaging, Photoacoustics. 14 (June 8) (2019) 77–98, 10.1016/j.pacs.2019.05.001 eCollection 2019 Jun. Review. [PubMed: 31293884]

[33]. Zackrisson S, van de Ven SMWY, Gambhir SS, Light in and sound out: emerging translational strategies for photoacoustic imaging, Cancer Res. 74 (February (4)) (2014) 979–1004. [PubMed: 24514041]

[34]. Zhu Q, Ricci A Jr., Hegde P, Kane M, Cronin E, Merkulov A, Xu Y, Tavakoli B, Tannenbaum S, Assessment of functional differences in malignant and benign breast lesions and improvement of diagnostic accuracy by using US-guided diffuse optical tomography in conjunction with conventional US, Radiology 280 (August (2)) (2016) 387–397, 10.1148/radiol.2016151097 Epub 2016 Mar 2. [PubMed: 26937708]

[35]. Neuschler EI, Butler R, Young CA, Barke LD, Bertrand ML, Böhm-Vélez M, Destounis S, Donlan P, Grobmyer SR, Katzen J, Kist KA, Lavin PT, Makariou EV, Parris TM, Schilling KJ, Tucker FL, Dogan BE, A pivotal study of optoacoustic imaging to diagnose benign and malignant breast masses: a new evaluation tool for radiologists, Radiology 287 (May (2)) (2018) 398–412, 10.1148/radiol.2017172228 Epub 2017 Nov 27. [PubMed: 29178816]

[36]. Folkman J, Tumor angiogenesis: therapeutic implications, NEJM 285 (1971) 1182–1186. [PubMed: 4938153]

[37]. Folkman J, Watson K, Ingber D, Hanahan D, Induction of angiogenesis during the transition from hyperplasia to neoplasia, Nature 339 (1989) 58–61. [PubMed: 2469964]

[38]. Paskilniskis MG, Wells WA, Schwab MC, et al. Tumor angiogenesis change estimated by using diffuse optical spectroscopic tomography: demonstrated correlation in women undergoing neoadjuvant chemotherapy for invasive breast cancer? Radiology (2011).

[39]. Ren K, Bal G, Hielscher AH, Frequency domain optical tomography based on the equation of radiative transfer, Siam J. Sci. Comput 28 (4) (2020) 1463–1489.

[40]. O'Leary MA, Boas DA, Chance B, Yodh AG, Experimental images of heterogeneous turbid media by frequency-domain diffusing-photon tomography, Opt. Lett 20 (5) (2020) 426–428.

[41]. Pifferi A, Swartling J, Chikoidze E, Torricelli A, Taroni P, Bassi A, Andersson-Engels S, Cubeddu R, Spectroscopic time-resolved diffuse reflectance and transmittance measurements of the female breast at different interfiber distances, J. Biomed. Opt 9 (November-December (6)) (2004) 1143–1151. [PubMed: 15568934]

[42]. Pifferi A, Contini D, Mora AD, Farina A, Spinelli L, Torricelli A, New frontiers in time-domain diffuse optics, a review, J. Biomed. Opt 21 (September (9)) (2016) 091310, 10.1117/1.JBO.21.9.091310. [PubMed: 27311627]

[43]. Grosenick D, Rinneberg H, Cubeddu R, Taroni P, Review of optical breast imaging and spectroscopy, J. of Biomed. Optics 21 (9) (2016) 091311.

[44]. Pogue B, Testorf M, McBride T, Osterberg U, Paulsen K, Instrumentation and design of a frequency-domain diffuse optical tomography imager for breast cancer detection, Opt. Express 22 (December (13)) (1997) 391–403.

[45]. Franceschini MA, Moesta KT, Fantini S, Gaida G, Gratton E, Jess H, Mantulin WW, Seeber M, Schlag PM, Kaschke M, Frequency-domain techniques enhance optical mammography: initial clinicalresults, Proc. Natl. Acad. Sci. U. S. A 94 (June (12)) (1997) 6468–6473. [PubMed: 9177241]

[46]. Siegel AM, Marota JJA, Boas DA, Design and evaluation of a continuous-wave diffuse optical tomography system, Optics Express 4 (8) (1999) 287–298, 10.1364/OE.4.000287. [PubMed: 19396285]

[47]. Flexman ML, Kim HK, Gunther JE, Lim EA, Alvarez MC, Desperito E, Kalinsky K, Hershman DL, Hielscher AH, Optical biomarkers for breast cancer derived from dynamic diffuse optical tomography, J. Biomed. Opt 18 (September (9)) (2013) 096012, 10.1117/1.JBO.18.9.096012. [PubMed: 24048367]

[48]. Schmitz CH, Klemer DP, Hardin R, Katz MS, Pei Y, Graber HL, Levin MB, Levina RD, Franco NA, Solomon WB, Barbour RL, Design and implementation of dynamic near-infrared optical tomographic imaging instrumentation for simultaneous dual-breast measurements, Appl. Opt 44 (11) (2005) 2140–2153. [PubMed: 15835360]

[49]. Li C, Zhao H, Anderson B, Jiang H, Multispectral breast imaging using a ten-wavelength, 64 × 64 source/detector channels silicon photodiode-based diffuse optical tomography system, Med. Phys 33 (March (3)) (2006) 627–636. [PubMed: 16878566]

[50]. El-Ghussein F, et al. Hybrid photomultiplier tube and photodiode parallel detection array for wideband optical spectroscopy of the breast guided by magnetic resonance imaging, J. Biomed. Opt 19 (1) (2014) 11010.

[51]. Uddin KMS, Mostafa A, Anastasio M, Zhu Q, Two step imaging reconstruction using truncated pseudoinverse as a preliminary estimate in ultrasound guided diffuse optical tomography, Biomed. Opt. Express 8 (November (12)) (2017) 5437–5449, 10.1364/BOE.8.005437 eCollection 2017 Dec 1. [PubMed: 29296479]

[52]. Li X, Heldermon CD, Yao L, Xi L, Jiang H, High resolution functional photoacoustic tomography of breast cancer, Med. Phys 42 (September (9)) (2015) 5321–5328, 10.1118/1.4928598. [PubMed: 26328981]

[53]. Heijblom M, et al. The state of the art in breast imaging using the twente photoacoustic mammoscope: results from 31 measurements on malignancies, Eur. Radiol 26 (11) (2016) 3874–3887. [PubMed: 26945762]

[54]. Fakhrejahani E, Torii M, Kitai T, Kanao S, Asao Y, Hashizume Y, Mikami Y, Yamaga I, Kataoka M, Sugie T, Takada M, Haga H, Togashi K, Shiina T, Toi M, Clinical report on the first prototype of a photoacoustic tomography system with dual illumination for breast cancer imaging, PLoS One 10 (October (10)) (2015) e0139113, 10.1371/journal.pone.0139113 eCollection 2015. [PubMed: 26506106]

[55]. Shiina T, Toi M, Yagi T, Development and clinical translation of photoacoustic mammography, Biomed. Eng. Lett 8 (May (2)) (2018) 157–165, 10.1007/s13534-018-0070-7 eCollection 2018 May. [PubMed: 30603200]

[56]. Lin L, Hu P, Shi J, Appleton CM, Maslov K, Li L, Zhang R, Wang LV, Single-breath-hold photoacoustic computed tomography of the breast, Nat. Commun 9 (June (1)) (2018) 2352, 10.1038/s41467-018-04576-z. [PubMed: 29907740]

[57]. Ermilov SA, Khamapirad T, Conjusteau A, Leonard MH, Lacewell R, Mehta K, et al. Laser optoacoustic imaging system for detection of breast cancer, J. Biomed. Opt 14 (2009) 024007. [PubMed: 19405737]

[58]. Diot G, Metz S, Noske A, Liapis E, Schroeder B, Ovsepian SV, Meier R, Rummeny E, Ntziachristos V, Multispectral optoacoustic tomography (MSOT) of human breast cancer, Clin. Cancer Res 23 (November (22)) (2017) 6912–6922, 10.1158/1078-0432.CCR-16-3200 Epub 2017 Sep 12. [PubMed: 28899968]

[59]. Deán-Ben XL, Fehm TF, Gostic M, Razansky D, Volumetric hand-held optoacoustic angiography as a tool for real-time screening of dense breast, J. Biophotonics 9 (March (3)) (2016) 253–259, 10.1002/jbio.201500008 Epub 2015 May 12. [PubMed: 25966021]

[60]. Becker A, Masthoff M, Claussen J, Ford SJ, Roll W, Burg M, Barth PJ, Heindel W, Schäfers M, Eisenblätter M, Wildgruber M, Multispectral optoacoustic tomography of the human breast: characterisation of healthy tissue and malignant lesions using a hybrid ultrasound-optoacoustic approach, Eur. Radiol 28 (February (2)) (2018) 602–609, 10.1007/s00330-017-5002-x Epub 2017 Aug 7. [PubMed: 28786007]

[61]. Oraevsky AA, Clingman B, Zalev J, Stavros AT, Yang WT, Parikh JR, Clinical optoacoustic imaging combined with ultrasound for coregistered functional and anatomical mapping of breast tumors, Photoacoustics 12 (August 31) (2018) 30–45, 10.1016/j.pacs.2018.08.003 eCollection 2018 Dec.. [PubMed: 30306043]

[62]. Grosenick D, Wabnitz H, Rinneberg HH, Moesta KT, Schlag PM, Development of a time-domain optical mammograph and first in vivo applications, Appl. Opt 38 (13) (1999) 2927. [PubMed: 18319875]

[63]. Taroni P, Danesini G, Torricelli A, Pifferi A, Spinelli L, Cubeddu R, Clinical trial of time-resolved scanning optical mammography at 4 wavelengths between 683 and 975 nm, J. Biomed. Opt 9 (3) (2004) 464–473. [PubMed: 15189083]

[64]. Choe R, Konecky SD, Corlu A, Lee K, Durduran T, Busch DR, Pathak S, Czerniecki BJ, Tchou J, Fraker DL, Demichele A, Chance B, Arridge SR, Schweiger M, Culver JP, Schnall MD, Putt ME, Rosen MA, Yodh AG, Differentiation of benign and malignant breast tumors by in-vivo three-dimensional parallel-plate diffuse optical tomography, J. Biomed. Opt 14 (March-April (2)) (2009) 024020, 10.1117/1.3103325. [PubMed: 19405750]

[65]. Yu Y, Liu N, Sassaroli A, Fantini S, Near-infrared spectral imaging of the female breast for quantitative oximetry in optical mammography, Appl. Opt 48 (10) (2009) D225–D235. [PubMed: 19340113]

[66]. Intes X, et al. Time-domain optical mammography softscan: initial results, Acad. Radiol 12 (8) (2005) 934–947. [PubMed: 16023382]

[67]. Poplack SP, Tosteson TD, Wells WA, Pogue BW, Meaney PM, Hartov A, Kogel CA, Soho SK, Gibson JJ, Paulsen KD, Electromagnetic breast imaging: results of a pilot study in women with abnormal mammograms, Radiology 243 (2007) 350–359. [PubMed: 17400760]

[68]. Enfield LC, Gibson AP, Everdell NL, Delpy DT, Schweiger M, Arridge SR, Richardson C, Keshtgar M, Douek M, Hebden JC, Three-dimensional time-resolved optical mammography of the uncompressed breast, Appl. Opt 46 (17) (2007) 3628–3638. [PubMed: 17514325]

[69]. Tromberg BJ, Cerussi A, Shah N, Compton M, Durkin A, Hsiang D, Butler J, Mehta R, Imaging in breast cancer: diffuse optics in breast cancer: detecting tumors in pre-menopausal women and monitoring neoadjuvant chemotherapy, Breast Cancer Res. 7 (6) (2005) 279–285. [PubMed: 16457705]

[70]. Chance B, Nioka S, Zhang J, Conant EF, Hwang E, Briest S, Orel SG, Schnall MD, Czerniecki BJ, Breast cancer detection based on incremental biochemical and physiological properties of breast cancers: a six-year, two-site study, Acad. Radiol 12 (8) (2005) 925–933. [PubMed: 16023383]

[71]. Erickson SJ, Godavarty A, Hand-held based near-infrared optical imaging devices: a review, Med. Eng. Phys 31 (5) (2009) 495–509. [PubMed: 19054704]

[72]. Zhu Q, Chen N, Kurtzman SH, Imaging tumor angiogenesis by use of combined near-infrared diffusive light and ultrasound, Opt. Lett 28 (5) (2003) 337–339. [PubMed: 12659436]

[73]. Yalavarthy PK, Pogue BW, Dehghani H, Carpenter CM, Jiang S, Paulsen KD, Structural information within regularization matrices improves near infrared diffuse optical tomography, Opt. Express 15 (2007) 8043–8058. [PubMed: 19547132]

[74]. Zhang L, Zhao Y, Jiang S, Pogue BW, Paulsen KD, Direct regularization from co-registered anatomical images for MRI-guided near-infrared spectral tomographic image reconstruction, Biomed. optics express 6 (2015) 3618–3630.

[75]. Fang Q, Carp SA, Selb J, Boverman G, Zhang Q, Kopans DB, Moore RH, Miller EL, Brooks DH, Boas DA, Combined optical imaging and mammography of the healthy breast: optical

contrast derived from breast structure and compression, IEEE Trans. Med. Imaging 28 (January (1)) (2009) 30–42, 10.1109/TMI.2008.925082. [PubMed: 19116186]

[76]. Fang Q, Selb J, Carp SA, Boverman G, Miller EL, Brooks DH, Moore RH, Kopans DB, Boas DA, Combined optical and X-ray tomosynthesis breast imaging, Radiology 258 (January (1)) (2011) 89–97, 10.1148/radiol.10082176 Epub 2010 Nov 9. [PubMed: 21062924]

[77]. Michaelsen KE, Krishnaswamy V, Shi L, Vedantham S, Karellas A, Pogue BW, Paulsen KD, Poplack SP, Effects of breast density and compression on normal breast tissue hemodynamics through breast tomosynthesis guided near-infrared spectral tomography, J. Biomed. Opt 21 (Sep (9)) (2016) 91316, 10.1117/1.JBO.21.9.091316. [PubMed: 27677170]

[78]. Zhu Q, Huang M, Chen N, Zarfos K, Jagjivan B, Kane M, Hedge P, Kurtzman SH, Ultrasound-guided optical tomographic imaging of malignant and benign breast lesions: initial clinical results of 19 cases, Neoplasia 5 (September-October (5)) (2003) 379–388. [PubMed: 14670175]

[79]. Zhu Q, Cronin EB, Currier AA, Vine HS, Huang M, Chen N, Xu C, Benign versus malignant breast masses: optical differentiation with US-guided optical imaging reconstruction, Radiology 237 (October (1)) (2005) 57–66. [PubMed: 16183924]

[80]. Zhu Q, Hegde PU, Ricci A Jr., Kane M, Cronin EB, Ardeshirpour Y, Xu C, Aguirre A, Kurtzman SH, Deckers PJ, Tannenbaum SH, Early-stage invasive breast cancers: potential role of optical tomography with US localization in assisting diagnosis, Radiology 256 (Aug (2)) (2010) 367–378, 10.1148/radiol.10091237 Epub 2010 Jun 22. [PubMed: 20571122]

[81]. You SS, Jiang YX, Zhu QL, Liu JB, Zhang J, Dai Q, Liu H, Sun Q, US-guided diffused optical tomography: a promising functional imaging techniquein breast lesions, Eur. Radiol 20 (February (2)) (2010) 309–317, 10.1007/s00330-009-1551-y Epub 2009 Aug 26. [PubMed: 19707770]

[82]. Kim MJ, Kim JY, Youn JH, Kim MH, Koo HR, Kim SJ, Sohn YM, Moon HJ, Kim EK, US-guided diffuse optical tomography for breast lesions: the reliability of clinical experience, Eur. Radiol 21 (July (7)) (2011) 1353–1363, 10.1007/s00330-011-2060-3 Epub 2011 Jan 28. [PubMed: 21274716]

[83]. Zhi W, Gu X, Qin J, Yin P, Sheng X, Gao SP, Li Q, Solid breast lesions: clinical experience with US-guided diffuse optical tomography combined with conventional US, Radiology 265 (Nov (2)) (2012) 371–378, 10.1148/radiol.12120086 Epub 2012 Sep 25. [PubMed: 23012460]

[84]. Ntziachristos V, Yodh AG, Schnall M, Chance B, MRI-guided diffuse optical spectroscopy of malignant and benign breast lesions, Neoplasia 4 (Jul (4)) (2002) 347–354. [PubMed: 12082551]

[85]. Brooksby B, Pogue BW, Jiang S, Dehghani H, Srinivasan S, Kogel C, Tosteson TD, Weaver J, Poplack SP, Paulsen KD, Imaging breast adipose and fibroglandular tissue molecular signatures by using hybrid MRI-guided near-infrared spectral tomography, Proc. Natl. Acad. Sci. U. S. A 103 (23) (2006) 8828–8833. [PubMed: 16731633]

[86]. Mastanduno MA, Xu J, El-Ghussein F, Jiang S, Yin H, Zhao Y, Wang K, Ren F, Gui J, Pogue BW, Paulsen KD, MR-guided near-infrared spectral tomography increases diagnostic performance of breast MRI, Clin. Cancer Res 21 (September (17)) (2015) 3906–3912, 10.1158/1078-0432.CCR-14-2546 Epub 2015 May 27. [PubMed: 26019171]

[87]. Feng J, Xu J, Jiang S, Yin H, Zhao Y, Gui J, Wang K, Lv X, Ren F, Pogue BW, Paulsen KD, Addition of T2-guided optical tomography improves noncontrast breast magnetic resonance imaging diagnosis, Breast Cancer Res. 19 (October (1)) (2017) 117, 10.1186/s13058-017-0902. [PubMed: 29065920]

[88]. Krishnaswamy V, Michaelsen KE, Pogue BW, Poplack SP, Shaw I, Defrietas K, Brooks K, Paulsen KD, A digital x-ray tomosynthesis coupled near infrared spectral tomography system for dual-modality breast imaging, Opt. Express 20 (17) (2012) 19125–19136, 10.1364/OE.20.019125. [PubMed: 23038553]

[89]. Zimmermann BB, Deng B, Singh B, Martino M, Selb J, Fang Q, Sajjadi AY, Cormier J, Moore RH, Kopans DB, Boas DA, Saksena MA, Carp SA, Multimodal breast cancer imaging using coregistered dynamic diffuse optical tomography and digital breast tomosynthesis, J. Biomed. Opt 22 (April (4)) (2017) 46008, 10.1117/1.JBO.22.4.046008. [PubMed: 28447102]

[90]. Vavadi H, Mostafa A, Zhou F, Uddin KMS, Althobaiti M, Xu C, Bansal R, Ademuyiwa F, Poplack S, Zhu Q, Compact ultrasound-guided diffuse optical tomography system for breast cancer imaging, J. Biomed. Opt 24 (October (2)) (2018) 1–9, 10.1117/1.JBO.24.2.021203.

[91]. Zhang Q, Brukilacchio TJ, Li A, Stott JJ, Chaves T, Hillman E, Wu T, Chorlton M, Rafferty E, Moore RH, Kopans DB, Boas DA, Coregistered tomographic x-ray and optical breast imaging: initial results, J. Biomed. Opt 10 (March-April (2)) (2005) 024033. [PubMed: 15910106]

[92]. Michaelsen KE, Krishnaswamy V, Shi L, Vedantham S, Poplack SP, Karellas A, Pogue BW, Paulsen KD, Calibration and optimization of 3D digital breast tomosynthesis guided near infrared spectral tomography, Biomed. Opt. Express 6 (November (12)) (2015) 4981–4991, 10.1364/BOE.6.004981 eCollection 2015 Dec. [PubMed: 26713210]

[93]. Mastanduno MA, Xu J, El-Ghussein F, Jiang S, Yin H, Zhao Y, Wang K, Ren F, Gui J, Pogue BW, Paulsen KD, MR-guided near-infrared spectral tomography increases diagnostic performance of breast MRI, Clin. Cancer Res 21 (September (17)) (2015) 3906–3912, 10.1158/1078-0432.CCR-14-2546 Epub 2015 May 27. [PubMed: 26019171]

[94]. Feng J, Xu J, Jiang S, Yin H, Zhao Y, Gui J, Wang K, Lv X, Ren F, Pogue BW, Paulsen KD, Addition of T2-guided optical tomography improves noncontrast breast magnetic resonance imaging diagnosis, Breast Cancer Res. 19 (Oct (1)) (2017) 117, 10.1186/s13058-017-0902. [PubMed: 29065920]

[95]. Zhu Q, You S, Jiang Y, Zhang J, Xiao M, Dai Q, Sun Q, Detecting angiogenesis in breast tumors: comparison of color Doppler flow imaging with ultrasound-guided diffuse optical tomography, Ultrasound Med. Biol 37 (Junuary (6)) (2011) 862–869, 10.1016/j.ultrasmedbio.2011.03.010 Epub 2011 Apr 30. [PubMed: 21531497]

[96]. Choi JS, Kim MJ, Youk JH, Moon HJ, Suh HJ, Kim EK, US-guided optical tomography: correlation with clinicopathologic variables in breast cancer, Ultrasound Med. Biol 39 (February (2)) (2013) 233–240, 10.1016/j.ultrasmedbio.2012.09.014 Epub 2012 Dec 4. [PubMed: 23219038]

[97]. Kim MJ, Su MY, Chen JH Yu HJ, Kim EK, Moon HJ, Choi JS, US-localized diffuse optical tomography in breast cancer: comparison with pharmacokinetic parameters of DCE-MRI and with pathologic biomarkers, BMC Cancer 16 (February 1) (2016) 50, 10.1186/s12885-016-2086-7. [PubMed: 26833069]

[98]. Zhi W, Wang Y, Chang C, Wang F, Chen Y, Hu N, Zhu X, Xie L, US-guided diffuse optical tomography: clinicopathological features affect total hemoglobin concentration in breast cancer, What Transl Oncol 11 (August (4)) (2018) 845–851, 10.1016/j.tranon.2018.04.009 Epub 2018 May 9. [PubMed: 29753185]

[99]. Asao Y, Hashizume Y, Suita T, Nagae KI, Fukutani K, Sudo Y, Matsushita T, Kobayashi S, Tokiwa M, Yamaga I, Fakhrejahani E, Torii M, Kawashima M, Takada M, Kanao S, Kataoka M, Shiina T, Toi M, Photoacoustic mammography capable of simultaneously acquiring photoacoustic and ultrasound images, J. Biomed. Opt 21 (November (11)) (2016) 116009, 10.1117/1.JBO.21.11.116009. [PubMed: 27893089]

[100]. Neuschler EI, Lavin PT, Tucker FL, Barke LD, Bertrand ML, Böhm-Vélez M, Destounis S, Dogan BE, Grobmyer SR, Katzen J, Kist KA, Makariou EV, Parris TM, Young CA, Butler R, Downgrading and upgrading gray-scale ultrasound BI-RADS categories of benign and malignant masses with optoacoustics: a pilot study, AJR Am. J. Roentgenol 211 (September (3)) (2018) 689–700, 10.2214/AJR.17.18436 Epub 2018 Jul 5. [PubMed: 29975115]

[101]. Menezes GLG, Pijnappel RM, Meeuwis C, Bisschops R, Veltman J, Lavin PT, van de Vijver MJ, Mann RM, Downgrading of breast masses suspicious for cancer by using optoacoustic breast imaging, Radiology 288 (August (2)) (2018) 355–365, 10.1148/radiol.2018170500 Epub 2018 Apr 17. [PubMed: 29664342]

[102]. Butler R, Lavin PT, Tucker FL, Barke LD, Böhm-Vélez M, Destounis S, Grobmyer SR, Katzen J, Kist KA, Makariou EV, Schilling KJ, Young CA, Dogan BE, Neuschler EI, Optoacoustic breast imaging: imaging-pathology correlation of optoacoustic features in benign and malignant breast, Masses 211 (November (5)) (2018) 1155–1170, 10.2214/AJR.17.18435 Epub 2018 Aug 14.

[103]. Joshi BP, Wang TD, Targeted optical imaging agents in cancer: focus on clinical applications, Contrast Media Mol. Imaging 2018 (August 27) (2018) 2015237, 10.1155/2018/2015237 eCollection 2018. [PubMed: 30224903]

[104]. Chitgupi U, Nyayapathi N, Kim J, Wang D, Sun B, Li C, Carter K, Huang WC, Kim C, Xia J, Lovell JF, Surfactant-stripped micelles for NIR-II photoacoustic imaging through 12 cm of breast

tissue and whole human breasts, Adv Mater. 31 (October (40)) (2019) e1902279, 10.1002/adma.201902279 Epub 2019 Aug. [PubMed: 31414515]

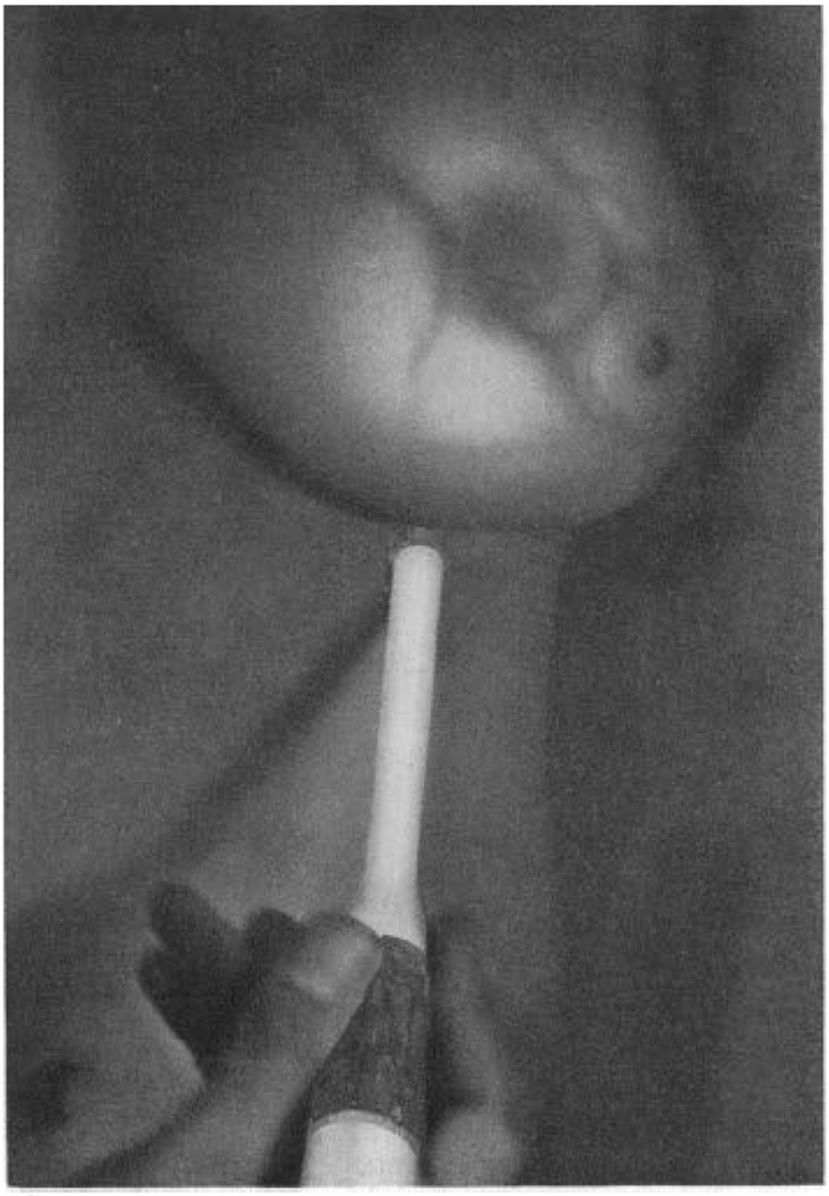

FIG. 2.—Opacity on transillumination of a solid tumor in the breast.

Fig. 1.
Transillumination of the Breast from Fig. 2 in Cutler M. Ann Surg. 1931;93(1):223–34.

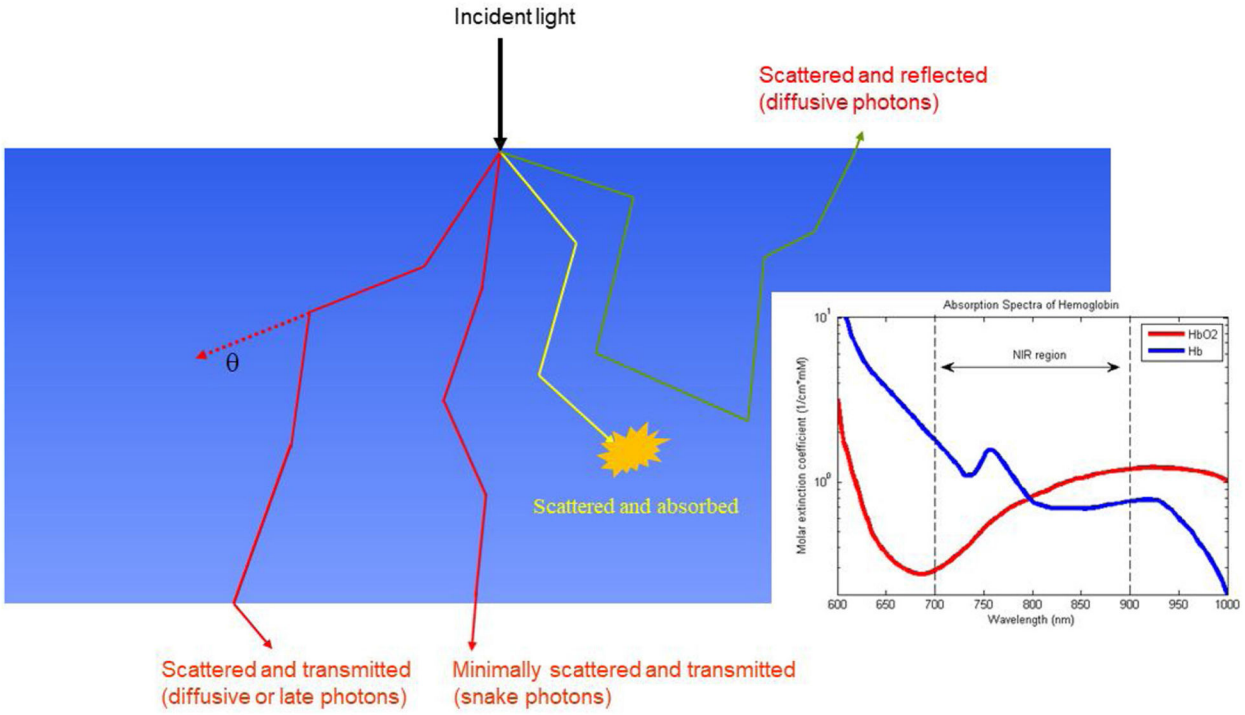

Fig. 2.

Illustration of photon propagation in biological tissue. Most photons received from the breast tissue either in transmit or reflection geometry emanate from scattering. Oxygenated and deoxygenated hemoglobin absorption spectrum is shown in the insert [commons.wikimedia.org].

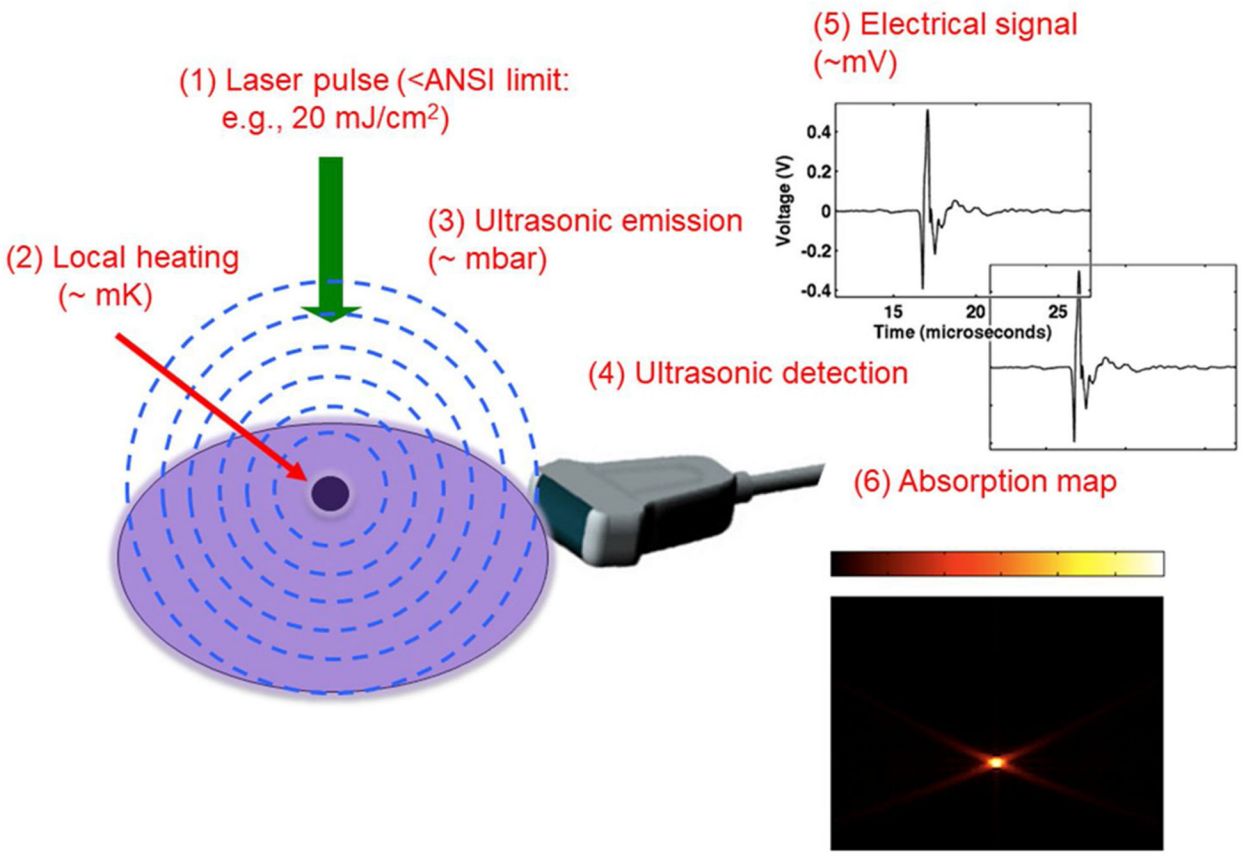

Fig. 3.

Illustration of photoacoustic signal generation. Short nanoseconds laser pulses are directly to the tissue and the absorption of the laser pulses by a lesion generates acoustic or photoacoustic waves that can be detected by an US array. The spatial measurements of the photoacoustic waves can be used to generate a lesion map which is directly related to lesion vascular network.

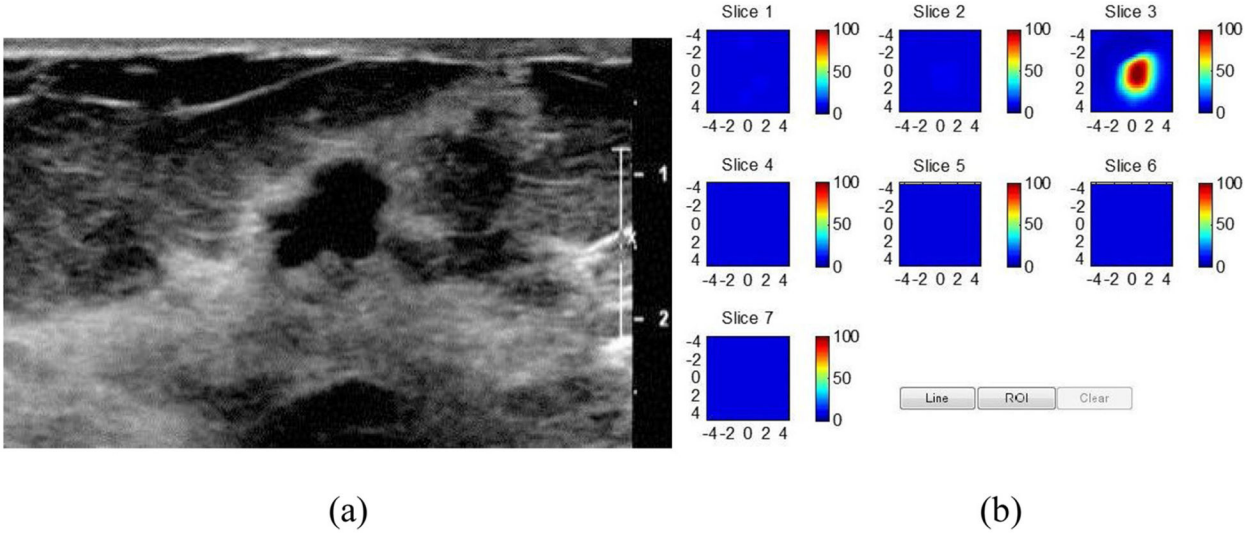

Fig. 4.

US-guided DOT of 6 mm intermediate grade DCIS with cribiform architecture. a. Gray scale US demonstrating an irregular mass with indistinct margins. b. DOT derived total Hemoglobin (THb) map reveals a localized distribution of THb in the malignant range, (maximum THB = 106 μM.). The map is comprised of 7 successive coronal imaging planes from 0.5 cm −3.5 cm from the skin with a vertical scale of THb concentration in μM. (from Zhu et al, Radiol 2016).

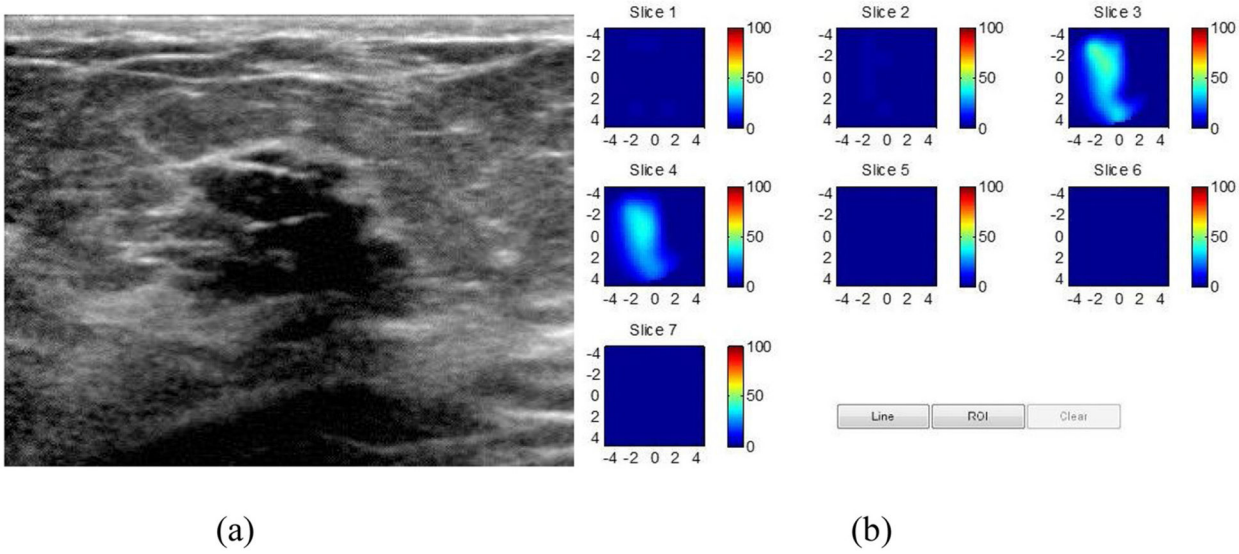

Fig. 5.

US- guided DOT of a hyalinized fibroadenoma. **(a)** Gray scale US image demonstrating an oval mass with microlobulated margins. (b) DOT derived THb map showing a diffuse distribution with a maximum THb of 53 μM in the probably benign range. (From Zhu et al, Radiol 2016).

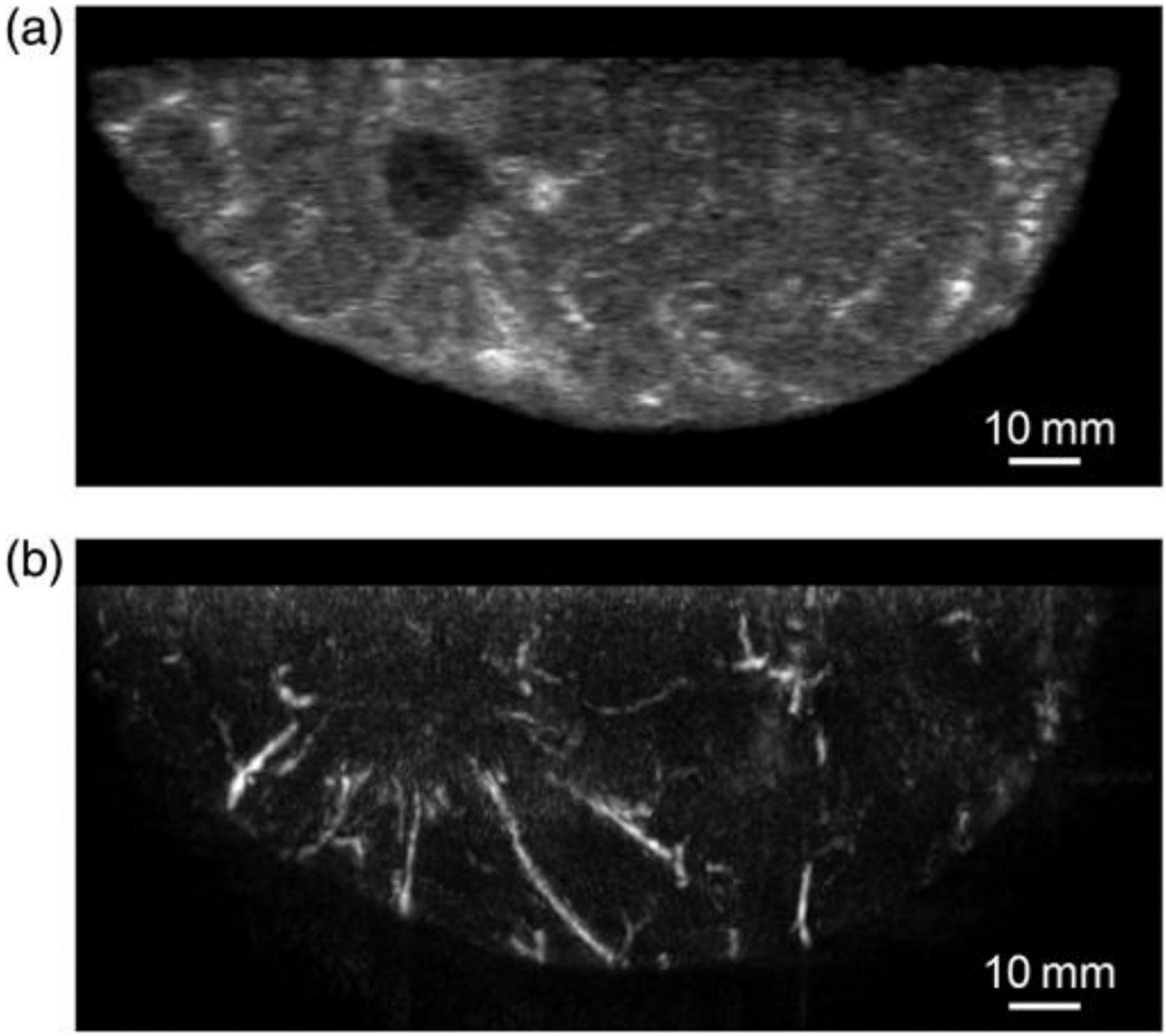

Fig. 6.

A 44-year-old woman with an invasive ductal carcinoma of 3.0 cm measured by US. (a) US image obtained by co-registered US and PAI system and (b) PAI image simultaneously obtained with US showing many blood vessel-like signals around the solid lesion seen by US [From Asao et al. J Biomed Opt. 2016]

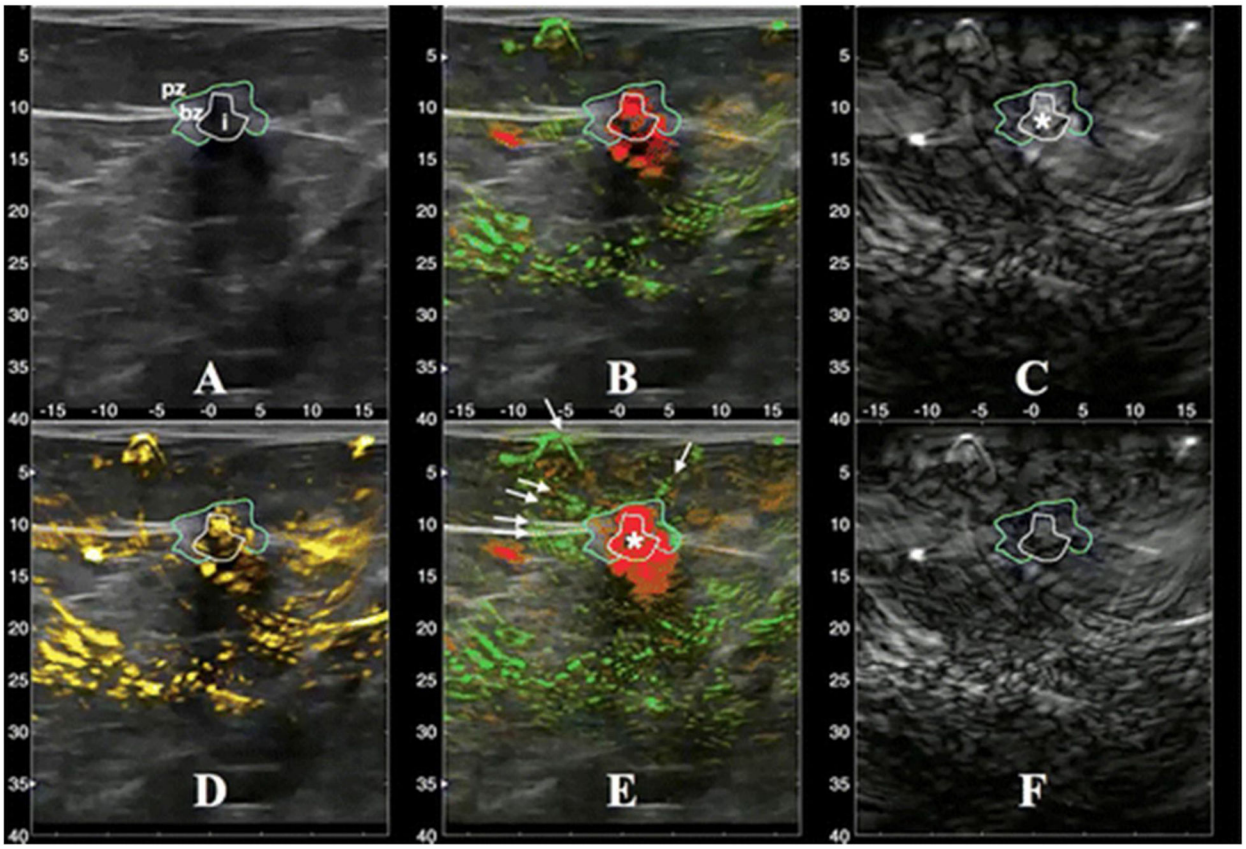

Fig. 7.

A 6-mm invasive ductal and lobular carcinoma. A: Grayscale US image. B: The PAT combined map shows relatively oxygenated blood as green and relatively deoxygenated blood as red. C: Short wave (755 nm) map displayed in gray scale. D: The total hemoglobin map. E: Similar to B and may have different threshold. F: Long wave (1064 nm.) map displayed in gray scale. Segmentation lines were manually drawn on the US image and propagated to co-registered locations on the five maps (B-F) to help distinguish distributions of PAT findings. (From Neuschler et al, Radiol 2018).

Table 1

DBT and MRI guided DOT clinical trials performed in > 20 subjects and including women with breast abnormalities.

Imaging Modality	1 st Author	Year Pub.	Patients {lesions}	Objectives	Key Results
DBT	Fang, Q.	2011	125 {189}	Explore the **optical** and physiologic properties of normal and lesion-bearing breasts	Bulk tissue THb (n = 138 normal breasts) 19.2 μM and sO2 0.73. Cancer THb (n = 26) significantly greater than fibroglandular tissue of the same breast (P=.0062). Solid benign lesions (n=17) and cysts (n = 8) significantly lower THb than cancers (P = .025 and P = .0033, respectively).
CEMRI-	Mastanduno, MA.	2015	30	Differentiation benign vs. malignant abnormalities, operating characteristics	THb and TOI*: sig differences cancer vs. benign, combined MRI & TOI: AUC 0.95, sens 95 %, spec 89 %, PPV 95 %, NPV 89 %
CEMRI, MRI (T2, DWI)	Feng, J.	2017	24	Operating characteristics: (T2,DWI) MRI-DOT vs. CEMRI-DOT vs. CEMRI	CEMRI: AUC 0.81, sens 94 %, spec 63 %, acc 88 % T2-DWI T2-MRI DOT: AUC 0.95, sens 94 %, spec 100 %, acc 96 %, CEMRI-DOT: AUC .94, sens 88 %, spec 88 %, acc 88 %

Eur J Radiol. Author manuscript; available in PMC 2020 October 23.

Table 2

US guided DOT clinical trials performed in > 100 subjects.

1 st Author	Year Pub.	Patients {lesions}	Objectives	Key Results
Zhu, Qu	2010	162 {173}	Differentiating Tis/T1 vs T2–4 cancer vs. benign	Thb > 2x greater cancer vs. benign, US-DOT: T1 cancer, sens 92 %, spec 93 %, PPV 81 %, NPV 97 % T2–T4 cancer, sens 75 %, spec 93 %, PPV 69 %, NPV 95 % THb threshold of 82 μM
Zhu, Qu	2016	288 {297}	Quantify THb for a wide range of malignant and benign diseases Compare breast cancer diagnosis of conventional US, DOT alone and in conjunction with conventional US Correlation THb, HbO2 and Hb with histologic, nuclear grades	Conventional US and DOT, sens 96.6 %–100 %, spec 77.3 %–83.3 %, PPV 52.7 %–59.4 %, NPV 99.0 %–100 % THb moderately correlated with tumor histologic grade and nuclear grade; HbO2 moderately correlated with tumor nuclear grade THb threshold of 80μM THb lower threshold (THb < 50 μM) was employed, biopsy recommendations for 4A and 4B lesions decreased by an average of 45 %
You, SS	2010	198 {214}	THb cancer vs. benign, operating characteristic	US-DOT: sens 83.9 %, spec 66.7 %, acc 72.6 %, PPV 75.6 %, NPV 77.1 %
Zhu, Qi	2011	205 {214}		11 % cancers were non-vascular but had elevated THb; 26 % of benign lesions were vascular by color Doppler but low THb
			Color Doppler vs. US-DOT	THb threshold of 140μM
Kim, MJ	2011	111 {122}	Inter-observer agreement	Interobserver agreement in BI-RADS final assessment with US and US-DOT (almost perfect; $\kappa = 0.8618$) was improved compared with US alone (substantial agreement, $\kappa = 0.6574$). AUC under the ROC curve did not show significant differences between US and combined US and US-DOT
Zhi, W	2012	102 {136}	Compare conventional US and US-guide DOT in differentiating malignant solid breast lesions vs. benign.	US and US-DOT: Sens 100 %, spec 93.9 %, PPV 91.5 %, 100 %, Acc 96.3 %
Zhi, W	2018	447 {455}	To investigate THC characteristics and its association with clinical pathologic findings	THb significantly greater in ER−, PR− than in ER+, PR + cancers ($p = .005$ and $p = .01$, respectively) and that cancers with axillary lymph node metastases or lymphovascular invasion had higher average THb ($p = .042$ and $p = .043$, respectively).

Eur J Radiol. Author manuscript; available in PMC 2020 October 23.